doi: 10.4149/gpb_2022027

Urotensin II activates the ferroptosis pathway through circ0004372/miR-124/SERTAD4 to promote the activation of vascular adventitial fibroblasts

Yan-chao Hu, Tuo Han, Ya-jie Fan, Chun-yan Zhang, Yan Zhang, Wei-dong Ma and Cong-xia Wang

Department of Cardiovascular Medicine, The Second Affiliated Hospital of Xi'an Jiaotong University, Xi'an, China

Abstract. Both vascular adventitial fibroblasts (VAFs) and urotensin II (UII) play important roles in vascular remodeling diseases, but the mechanism of UII in VAFs is still unclear. UII inhibited miR-124 expression through up-regulating circ0004372 expression, thereby promoting SERTAD4 expression. UII significantly promoted the generation of ROS, MDA and 4-HNE, reduced the activities of SOD, GST and GR, increased Fe^{2+} concentration and inhibited GPX4 expression through circ0004372/miR-124/SERTAD4. Both UII and ferroptosis inducer Erastin significantly promoted the expression of α-SMA, Collagen I and TGF-β1 in VAFs, but circ0004372 siRNA, miR-124 mimics, SERTAD4 siRNA or Ferrostatin-1 significantly inhibited the effect of UII and Erastin on cell activation. When co-transfected with circ0004372 siRNA and miR-124 inhibitors or miR-124 mimics and SERTAD4 overexpression vector, UII still significantly increased the expression of α-SMA, Collagen I and TGF-β1. After transfection with circ0004372 overexpression vector, miR-124 inhibitors or SERTAD4 overexpression vector and then treating with UII and Ferrostatin-1, the expression of α-SMA, Collagen I and TGF-β1 was still significant; when the circ0004372 overexpression vector and miR-124 mimics or miR-124 inhibitors and SERTAD4 siRNA were co-transfected and then UII and Ferrostatin-1 were added, the expression of α-SMA, Collagen I and TGF-β1 was not significantly increased. Therefore, these results indicate that UII promotes the activation of VAFs through the circ0004372/miR-124/SERTAD4/ferroptosis pathway.

Key words: Cardiovascular remodeling — Vascular adventitial fibroblasts — Urotensin II — circRNA — Ferroptosis

Introduction

Cardiovascular remodeling is an important pathophysiological basis for cardiovascular diseases such as hypertension, atherosclerosis and restenosis after percutaneous coronary intervention (Pasterkamp et al. 2000; Sekaran et al. 2017). Its core is cell proliferation and phenotypic transformation (Lu et al. 2018), but its mechanism has not been fully elucidated.

Correspondence to: Cong-xia Wang, 157# Xiwu Road, Xincheng District, Xi'an 710004, Shaanxi Province, P.R. China
E-mail: huyanchao081@163.com

In the past, the adventitia has long been considered to only play a role in nutrition of tunica media and vascular support, but recent studies have shown that adventitia also plays an important role in the process of cardiovascular remodeling (Tinajero and Gotlieb 2020). The main cells of adventitia are vascular adventitial fibroblasts (VAFs), which can be activated by a variety of factors to proliferate and migrate, and can produce and release a variety of vasoactive substances, thereby affecting and participating in the occurrence and development of vascular remodeling diseases (An et al. 2015). Our previous studies have found that urotensin II (UII) induces VAFs to secrete trans-

forming growth factor-beta1 (TGF-β1), thus promoting the phenotype differentiation of VAFs into myofibroblasts (Zhang et al. 2010). Subsequent studies have also confirmed that UII plays an important role in vascular remodeling diseases and is one of the current research hotspots in the cardiovascular field (Papadopoulos et al. 2008). However, there are few studies on the mechanism of UII activating VAFs.

Circular RNA (circRNA) is a special type of non-coding RNA discovered in recent years. It has important biological functions and can participate in the occurrence and development of various diseases such as nervous system diseases, cardiovascular diseases and cancer (Kristensen et al. 2019). At present, there has been some progress in the research of circRNA in cardiovascular diseases (Ding et al. 2018), but there is no research report on the role of circRNA in VAFs and its relationship with UII. Hsa_circ_0004372 (circ0004372) is a circRNA up-regulated in human thoracic aortic dissection (Zou et al. 2017). This study further found that its expression was induced by UII, indicating that the role of UII in VAFs is related to circ0004372. circ0004372 could regulate the expression of miR-124 and SERTA domain containing 4 (SERTAD4) in VAFs. miR-124 is down-regulated in pulmonary vascular fibroblasts in patients with pulmonary hypertension, and has the effect of inhibiting the activation of a variety of fibroblasts (Wang et al. 2014; Zhang et al. 2017). Stratton et al. (2019) found that TGF-β induced the expression of SERTAD4 to promote cardiac fibroblast activation. Therefore, miR-124 and SERTAD4 are both important fibrosis-related factors.

In addition, ferroptosis is a newly discovered way of cell death, and current studies have found that it is involved in the regulation of fibrosis process (Gong et al. 2019; Wang et al. 2020). However, whether ferroptosis affects the activation of VAFs has not yet been studied. Therefore, this study conducted a specific study on the relationship and role of UII/circ0004372/miR-124/SERTAD4 and ferroptosis pathway in VAFs, so as to provide more sufficient evidence for the biological function of VAFs.

Materials and Methods

Cell culture and target site prediction

Human aortic advential fibroblasts (Lonza, MD, USA) were cultured in Stromal Cell Medium (Lonza) containing 5% fetal bovine serum (FBS; Gibco, Carlsbad, CA, USA). VAFs were treated with 10^{-8} mol/l (M) of urotensin II (UII; Sigma-Aldrich, St Louis, MO, USA) for 24 h or stimulated with different concentrations of UII (10^{-10}–10^{-6} mol/l) for 0 to 48 h. RNAhybrid (https://bibiserv.cebitec.uni-bielefeld.de/rnahybrid/) was used to analyze the binding sites between circ0004372 or SERTAD4 and miR-124.

Cell transfection and quantitative real-time PCR (qRT-PCR)

SERTAD4 overexpression vector (SERTAD4-O) was obtained from GeneCopoeia (Guangzhou, China), and circ0004372 overexpression vector (circ0004372-O) was purchased from Geneseed (Guangzhou, China). SERTAD4 siRNA (5'-TCCTTAGAAAAGCTAAAGTTT-3'), circ0004372 siRNA (5'-ACGAAAGTTCCAGGAATGGAT-3'), miR-124 mimics and inhibitors, and negative control (NC) miRNA and siRNA (5'-AAGCGCGCTTTGUAGGATTCG-3') were synthesized by RiboBio (Guangzhou, China). When VAFs were seeded in 6-well plates (1×10^6 cells/well) and cultured to about 70% confluence, each plasmid (4 μg/well), siRNA and miRNA (50 nM/well) were transfected or co-transfected using X-tremeGENE 360 Transfection Reagent (Roche, Germany). After that, VAFs were treated with UII (10^{-8} mol/l), Erastin (10 μmol/l; Sigma-Aldrich), deferoxamine (DFO, 20 μmol/l; Sigma-Aldrich) or UII plus Ferrostatin-1 (Fer-1, 1 μmol/l; Sigma-Aldrich) or DFO for 24 h. A RNeasy Mini Kit (Qiagen, Germany) was used to extract total RNA from VAFs, and 1 μg of RNA was reverse transcribed into cDNA using All-in-One First-Strand cDNA Synthesis Kit (GeneCopoeia). RT-PCR was performed using the iQ SYBR Green Supermix (Bio-Rad, CA, USA) with equal amount of cDNA (2.5 ng). The reaction procedures described as followed: 5 min at 95°C; 30 cycles of 15 s at 95°C, 32 s at 60°C. The relative expression of genes was analyzed using the $2^{-\Delta\Delta Ct}$ method. The sequences of all primers were shown in Table 1.

Cell counting kit-8 (CCK-8) assay

VAFs were seeded into 96-well plates and then treated with different concentrations of UII. After that, VAFs were incubated with 10 μl CCK-8 solution (Beyotime, China) at 37°C for 2 h, and then the optical density (OD) value at 450 nm was tested using a microplate reader.

Subcellular fractionation location

The nuclear and cytoplasmic fractions of VAFs were extracted using a PARIS Kit (Invitrogen, CA, USA) according to the manufacturer's instructions. Briefly, VAFs were lysed with cell fractionation buffer and centrifuged to collect the supernatant containing the cytoplasmic fraction. Next, the nuclear pellet was lysed with cell disruption buffer. The nuclear lysate and cytoplasmic fraction were mixed with 2 × lysis/binding solution for RNA extraction, followed by reverse

transcription. The subcellular localization of circ0004372 was analyzed *via* qRT-PCR. U6 snRNA acted as nuclear control while 18S rRNA acted as cytoplasmic control.

RNA immunoprecipitation (RIP)

VAFs were lysed by RIP lysis buffer and used to perform RIP assay with a Magna RIP Kit (Millipore, Billerica, MA, USA). Magnetic beads coated with Anti-AGO2 antibody (Millipore) or negative control IgG (Millipore) were added into the cell lysates and then incubated for 3 h at 4°C. After that, circ0004372 enrichment in the precipitation was quantified *via* qRT-PCR.

Luciferase reporter assay

The wild-type (WT) or mutant (Mu) of full-length circ0004372 or SERTAD4-3' untranslated region (3' UTR) was cloned into the pmirGLO vector (Promega, Madison, WI, USA). The cells were co-transfected with luciferase reporter vector and miR-124 mimics or NC miRNA. After 48 h transfection, the luciferase activity was detected and normalized to Renilla luciferase activity using a Dual Glo Luciferase Assay System (Promega).

Western blot

VAFs were washed and then lysed using RIPA lysis buffer (Beyotime). The protein extracts were electrophoresed and transferred onto PVDF membranes (Millipore). After blockage with 10% nonfat milk, SERTAD4 (1:500; Novus Biologicals, CO, USA), glutathione peroxidase 4 (GPX4, 1:800; Cell Signaling Technology, Danvers, MA, USA), α-smooth muscle actin (α-SMA, 1:800; Cell Signaling Technology), Collagen I (1:800; Cell Signaling Technology) or GAPDH (1:1000; Cell Signaling Technology) primary antibody was added to the membranes. Then, membranes were incubated with secondary antibody (1: 5000; Cell Signaling Technology) and visualized using enhanced chemiluminescence (Beyotime).

Table 1. Primers for quantitative PCR

	Primer sequences
hsa_circ_0002271	F: 5'-TCAGATGCTGAAGCGAGTCC-3'
	R: 5'-CCCAGCATGACTGATAGTCCAA-3'
hsa_circ_0004372	F: 5'-TTGGTGCCCTCAACATCTCTC-3'
	R: 5'-GGGCTTCCAAATCCATTGACTC-3'
hsa_circ_0037909	F: 5'-ATGTATTTGACTGGAATGGTTGAC-3'
	R: 5'-CCCTGGCTCTGCTTCACTTA-3'
hsa_circ_0037911	F: 5'-TCATTGGGCACGTAGATGCT-3'
	R: 5'-TCTGAAAGTTCCATGCTAACAGC-3'
hsa_circ_0004104	F: 5'-ACCTGTGACCTGGACAATGAC-3'
	R: 5'-GGTGCACTTTGTGGCAAAGAA-3'
hsa-miR-124	F: 5'-ACACTCCAGCTGGGTAAGGCACGCGGTGAATG-3'
	R: 5'-CTCAACTGGTGTCGTGGA-3'
hsa-miR-124 RT	5'-CTCAACTGGTGTCGTGGAGTCGGCAATTCAGTTGAGTTGGCATT-3'
18S rRNA	F: 5'-CCAGTAAGTGCGGGTCATAAG-3'
	R: 5'-GGCCTCACTAAACCATCCAA-3'
U6	F: 5'-CTCGCTTCGGCAGCACA-3'
	R: 5'-AACGCTTCACGAATTTGCGT-3'
SERTAD4	F: 5'-CTGGCAGGATCACATTAC-3'
	R: 5'-CCTCTTCTTCCACATACTTC-3'
GPX4	F: 5'-GTGGAAGTGGATGAAGAT-3'
	R: 5'-GATGAGGAACTTGGTGAA-3'
α-SMA	F: 5'-GCGTGGCTATTCCTTCGTTA-3'
	R: 5'-ATGAAGGATGGCTGGAACAG-3'
Collagen I	F: 5'-GCTCTCCTGGTGAACAAG-3'
	R: 5'-ACCGTTGAGTCCATCTTTG-3'
GAPDH	F: 5'-GGTATCGTGGAAGGACTC-3'
	R: 5'-GTAGAGGCAGGGATGATG-3'

F, forward primer; R, reverse primer.

Measurement of intracellular ROS

The reactive oxygen species (ROS) level in cell samples was analyzed in triplicate using the OxiSelect In Vitro ROS/RNS Assay Kit (Cell Biolabs; San Diego, CA, USA) according to the manufacturer's instructions. Firstly, VAFs were mixed with 50 μl of Catalyst and incubated at room temperature for 5 min. Then 100 μl of dichlorodihydrofluorescin (DCFH) solution was added and incubated in dark for 30 min. After that, read the fluorescence with a fluorescence plate reader at 480 nm excitation/530 nm emission. Meanwhile, ROS probe DCFH-DA (Beyotime) was used to detect the generation of intracellular ROS. VAFs were washed twice with PBS, incubated with 20 μmol/l DCFH-DA in the dark for 30 min, and then dissolved with 1% Triton X-100. Finally, the fluorescence intensity was detected by fluorescence microscope.

Analysis of lipid peroxidation and Fe^{2+}

The malonaldehyde (MDA) concentration in cell lysates was determined using an MDA assay kit (Nanjing Jiancheng, China). Add 0.2 ml of MDA detection working solution to 0.1 ml of sample, mix well and heat at 100°C for 15 min. After centrifugation, the absorbance was measured at 532 nm with a microplate reader, and the MDA content was calculated. The concentration of 4-hydroxynonenal (4-HNE) in cell lysates was measured using the lipid peroxidation assay kit (Abcam, China) according to the kit instruction. Superoxide dismutase (SOD), glutathione S-transferases (GST) and glutathione reductase (GR) activities of VAFs were assessed with the SOD assay kit (Nanjing Jiancheng), GST activity detection kit (Solarbio, Beijing, China) and GR activity detection kit (Solarbio) according to the manufacturer's instructions. An Iron Assay Kit (Abcam) was used to detect the relative concentration of Fe^{2+} in cell lysates. After cell lysis, every 100 μl of sample was added with 5 μl of assay buffer, mixed well and incubate at 37°C for 30 min, and then the OD value of 593 nm was measured with a spectrophotometer.

Immunofluorescence staining and ELISA analysis

VAFs were fixed with 4% paraformaldehyde and permeabilized with 0.1% Triton X-100, and then blocked with 5% goat serum (Beyotime). After that, VAFs were incubated with anti-α-SMA (1:100, Abcam) overnight at 4°C, and then a secondary antibody (1:500, Abcam) were applied at room temperature for 1 h. The nuclei were stained with DAPI (Sigma-Aldrich) and cells were imaged with an Olympus fluorescence microscope (Japan). The supernatant of VAFs was harvested and used to detect the expression levels of Collagen I and TGF-β1 with a Collagen type I (COL1) (Human) ELISA Kit (BioVision, CA, USA) and TGF-β1 ELISA Kit (Beyotime).

Statistical analysis

SPSS 20.0 software (Chicago, IL, USA) and GraphPad Prism v8 (San Diego, CA, USA) were used for data analysis, and data from three independent experiments were expressed as mean ± SD. The analysis was carried out using a two-way analysis of variance (ANOVA) to compare between groups or an one-way ANOVA for multiple comparisons; $p < 0.05$ was considered significant.

Results

The function of circ0004372 induced by UII is related to miR-124

After stimulating VAFs with UII, detecting the expression of several cardiovascular disease-related circRNAs found that the expression of circ0004372 was significantly up-regulated (Fig. 1A). Further verification showed that UII promoted the expression of circ0004372 and VAFs viability in a concentration- and time-dependent manner (Fig. 1B–D), but with the further increase of UII concentration, circ0004372 expression was decreased (Fig. 1B). It may be due to high concentration of UII will activate other signal pathways to negatively regulate circ0004372, resulting in the inability to further increase circ0004372 expression. Similar phenomena exist for a variety of active molecules, such as UII (Zhang et al. 2008; Song et al. 2012; Yu et al. 2015) and angiotensin II (Ang II) (Shen et al. 2006). Therefore, the role of UII in VAFs may be related to circ0004372, which is worthy of in-depth study. Nuclear and cytoplasmic separation experiments showed that circ0004372 was mainly expressed in the cytoplasm and may have the effect of adsorbing miRNAs (Fig. 1E). Biological software analysis found that the sequence of circ0004372 contained the binding sites of miR-124 (Fig. 1F). RIP and dual luciferase reporter gene experiments showed that miR-124 could directly bind to circ0004372 (Fig. 1G and H), indicating that the function of circ0004372 is related to miR-124.

UII regulates the activation of circ0004372/miR-124/SERTAD4 pathway in VAFs

Further screening of miR-124 downstream target genes (Notch1, PTBP1, SERTAD4, AXIN1, RHOG, etc), among which SERTAD4 caught our attention. The sequence of SERTAD4 contained the binding site of miR-124 (Fig. 1F), and the dual luciferase reporter gene experiment also showed that miR-124 could bind to SERTAD4 (Fig. 2A). UII induced the expression of circ0004372 in VAFs and down-regulated the expression of miR-124; circ0004372 overexpression also inhibited the expression of miR-124, but down-regulation

of circ0004372 significantly attenuated the inhibitory effect of UII on miR-124 expression; when co-transfected with circ0004372 siRNA and miR-124 inhibitors, UII still significantly inhibited the expression of miR-124 (Fig. 2B and C). Simultaneous detection of SERTAD4 expression revealed that both UII and circ0004372 promoted the expression of SERTAD4, while miR-124 had the opposite effect; both circ0004372 siRNA and miR-124 mimics inhibited the effect of UII on the promotion of SERTAD4 expression; when co-transfected with circ0004372 siRNA and miR-124 inhibitors, UII still significantly promoted the expression of SERTAD4 (Fig. 2D and F). From the above results, it can be seen that UII regulates the expression of downstream miR-124 and SERTAD4 through circ0004372.

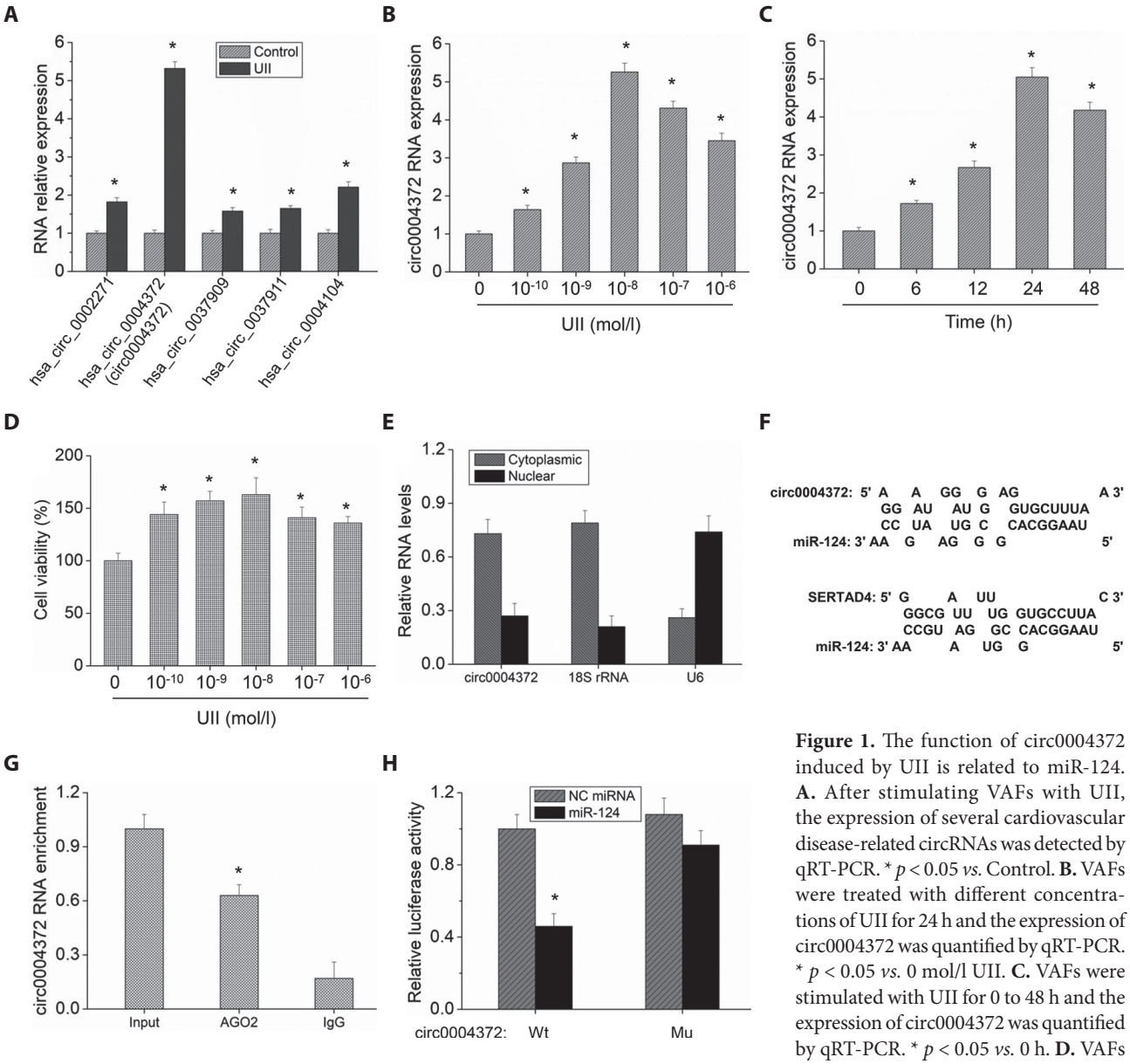

Figure 1. The function of circ0004372 induced by UII is related to miR-124. **A.** After stimulating VAFs with UII, the expression of several cardiovascular disease-related circRNAs was detected by qRT-PCR. * $p < 0.05$ *vs.* Control. **B.** VAFs were treated with different concentrations of UII for 24 h and the expression of circ0004372 was quantified by qRT-PCR. * $p < 0.05$ *vs.* 0 mol/l UII. **C.** VAFs were stimulated with UII for 0 to 48 h and the expression of circ0004372 was quantified by qRT-PCR. * $p < 0.05$ *vs.* 0 h. **D.** VAFs were treated with different concentrations of UII for 24 h and the cell viability was measured using CCK-8 assay. * $p < 0.05$ *vs.* 0 mol/l UII. **E.** The expression level of circ0004372 in nucleus and cytoplasm was detected by qRT-PCR. **F.** A potential binding site of miR-124 in circ0004372 and SERTAD4. **G.** The amount of circ0004372 enriched by anti-AGO2 was detected by RIP. * $p < 0.05$ *vs.* IgG. **H.** After co-transfection of luciferase reporter vector (200 ng/well) and miR-124 mimics (20 μmol/l), the binding relationship between circ0004372 and miR-124 was detected by dual luciferase reporter gene assay. * $p < 0.05$ *vs.* NC miRNA. UII, urotensin II; VAFs, vascular adventitial fibroblasts; WT, wild-type; Mu, mutant; NC, negative control.

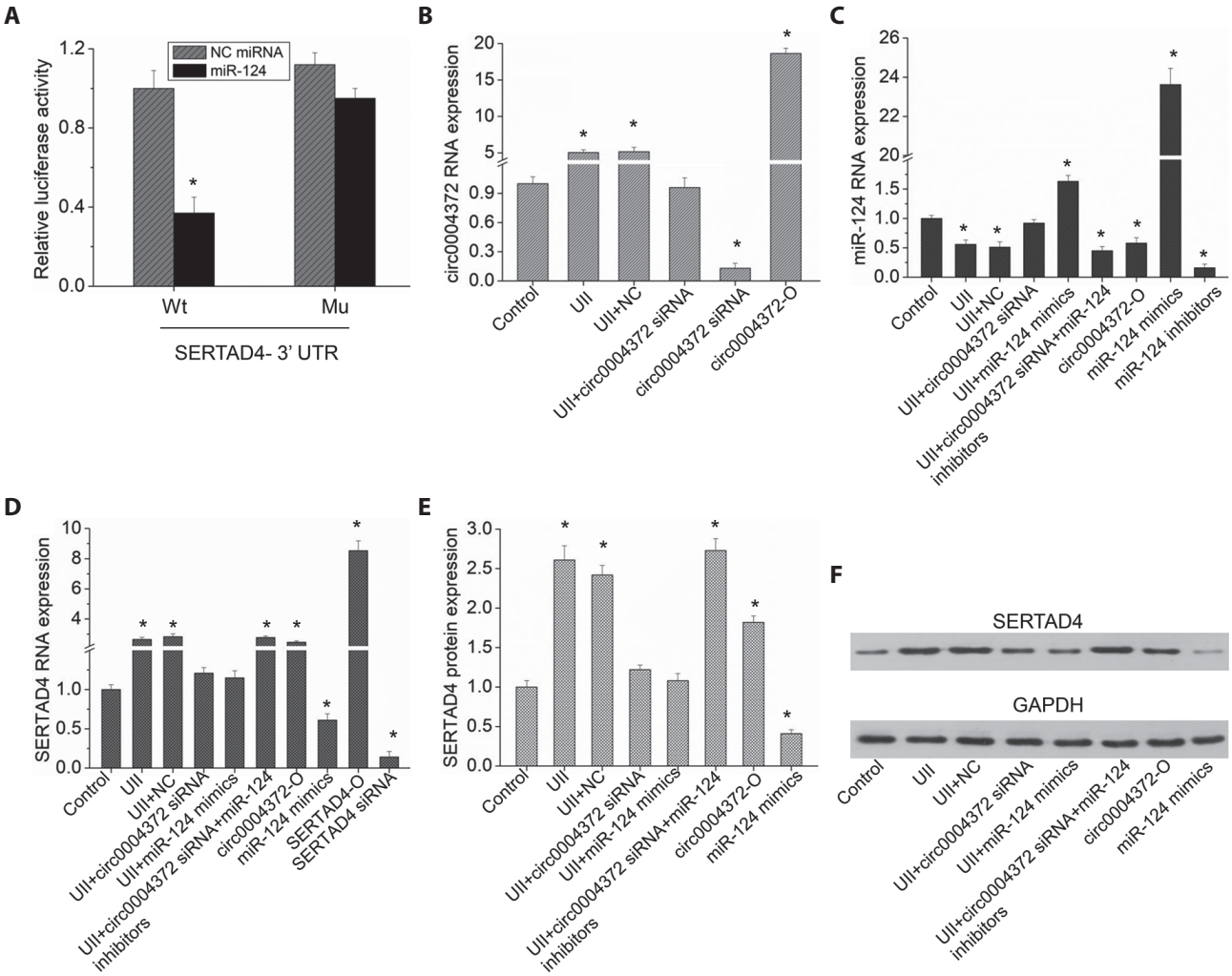

Figure 2. UII induces the expression of circ0004372 and then regulates the expression of miR-124 and SERTAD4 in VAFs. **A.** The binding relationship between SERTAD4 and miR-124 was detected by dual luciferase reporter gene assay. After transfection and/or treatment with UII, the expression of circ0004372 (**B**), miR-124 (**C**) and SERTAD4 (**D**) was tested by qRT-PCR. The protein expression level of SERTAD4 (**E**) was examined by Western blot (**F**). * $p < 0.05$ *vs.* NC miRNA or Control. For abbreviations, see Figure 1.

UII promotes ferroptosis of VAFs through the circ0004372/miR-124/SERTAD4 pathway

This study further explores whether UII/circ0004372/miR-124/SERTAD4 is involved in regulating the ferroptosis pathway. After stimulating VAFs with UII, the detection of ferroptosis-related indicators found that UII significantly promoted the production of ROS, MDA and 4-HNE (Fig. 3A–D), reduced the activities of SOD, GST and GR (Fig. 3E–G), increased the concentration of Fe^{2+} (Fig. 3H), and inhibited the expression of ferroptosis core regulatory factor GPX4 (Fig. 3I and J). circ0004372 siRNA, miR-124 mimics or SERTAD4 siRNA significantly blocked the role of UII in regulating ferroptosis related indicators; when co-transfected with circ0004372 siRNA and miR-124 inhibitors or miR-124 mimics and SERTAD4 overexpression vector, UII still significantly increased the content of ROS, MDA, 4-HNE and Fe^{2+}, reduced the activities of SOD, GST and GR, and inhibited the expression of GPX4 (Fig. 3). These results indicate that UII regulates the ferroptosis of VAFs through the circ0004372/miR-124/SERTAD4 pathway.

UII promotes the activation of VAFs through the circ0004372/miR-124/SERTAD4/ferroptosis pathway

Research continues to explore the role of UII/circ0004372/miR-124/SERTAD4/ferroptosis pathway in the activation of VAFs. UII significantly promoted the expression of α-SMA, Collagen I and TGF-β1 in VAFs (Fig. 4), indicating that UII can promote AF activation. circ0004372 siRNA, miR-124

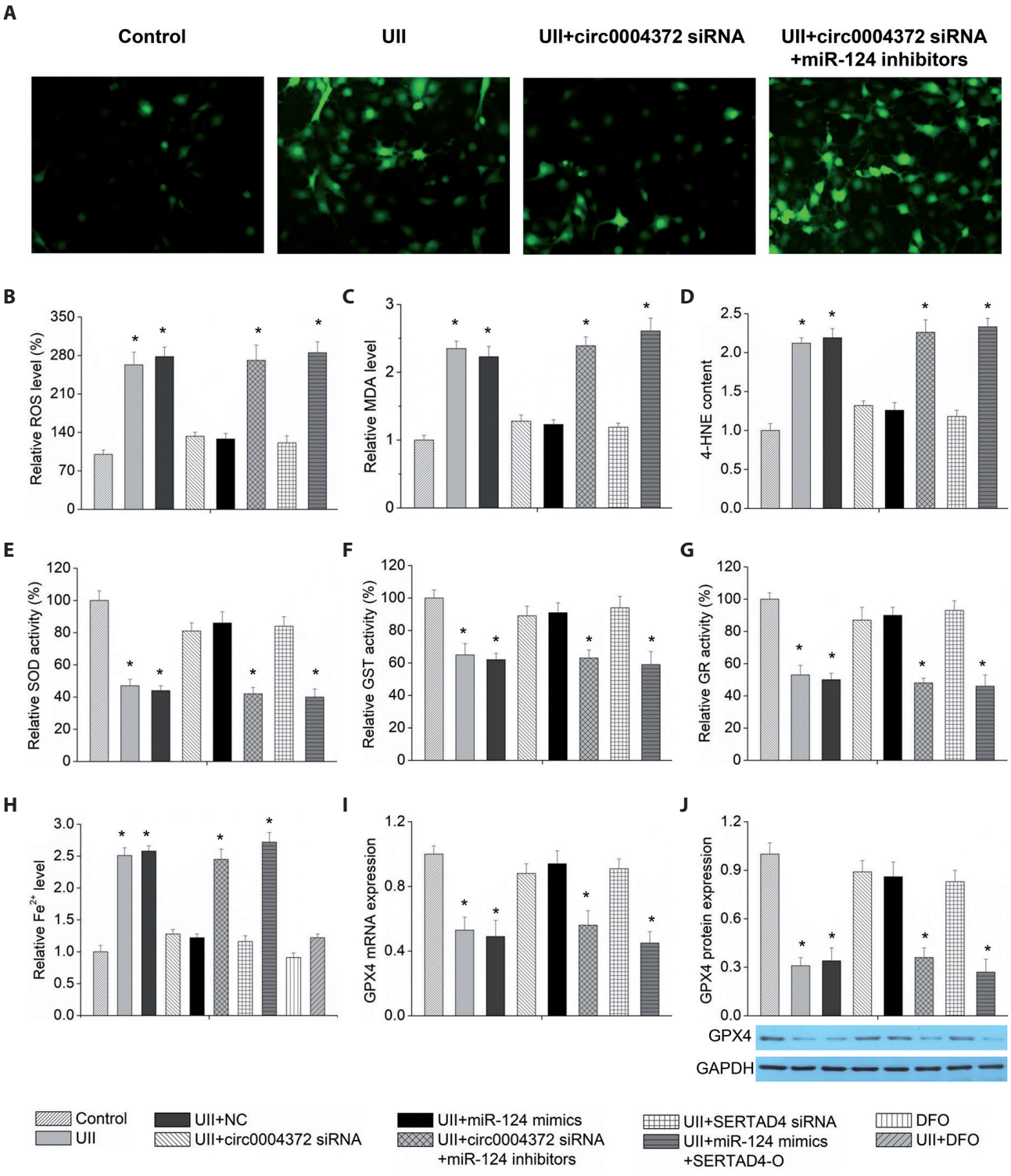

Figure 3. UII regulates VAFs ferroptosis through circ0004372/miR-124/SERTAD4 pathway. After transfection and then treatment with UII or only treatment with DFO or UII plus DFO, the generation of intracellular ROS was detected using ROS probe DCFH-DA (**A**), the levels of ROS (**B**), MDA (**C**), 4-HNE (**D**), SOD (**E**), GST (**F**), GR (**G**) and Fe^{2+} (**H**) were determined. The mRNA (**I**) and protein (**J**) expression levels of GPX4 were detected by qRT-PCR and Western blot. * $p < 0.05$ *vs.* Control. UII, urotensin II; VAFs, vascular adventitial fibroblasts; DFO, deferoxamine; ROS, reactive oxygen species; MDA, malonaldehyde; 4-HNE, 4-hydroxynonenal; SOD, superoxide dismutase; GST, glutathione S-transferases; GR, glutathione reductase.

mimics or SERTAD4 siRNA significantly inhibited the effect of UII on promoting cell activation; when co-transfected with circ0004372 siRNA and miR-124 inhibitors or miR-124 mimics and SERTAD4 overexpression vector, the expression of α-SMA, Collagen I and TGF-β1 was still increased significantly (Fig. 4). The above results indicate that UII promotes the activation of VAFs through the circ0004372/miR-124/SERTAD4 pathway.

When VAFs were treated with ferroptosis inducer Erastin, it was found that the expression of α-SMA, Collagen I and TGF-β1 was increased significantly (Fig. 5A–D), indicating that induction of ferroptosis can promote the activation of VAFs. circ0004372 siRNA, miR-124 mimics or SERTAD4 siRNA could also block the effect of Erastin on promoting cell activation; when co-transfected with circ0004372 siRNA and miR-124 inhibitors or miR-124 mimics and SERTAD4 overexpression vector, the effect of Erastin on promoting cell activation remained significant (Fig. 5A–D). Therefore, the circ0004372/miR-124/SERTAD4 pathway is involved in the regulation of ferroptosis activating VAFs.

When UII and the ferroptosis inhibitor Ferrostatin-1 (Fer-1) were added at the same time, the effect of UII on promoting the expression of α-SMA, Collagen I and TGF-β1 was inhibited (Fig. 5E–H), indicating that UII promotes the

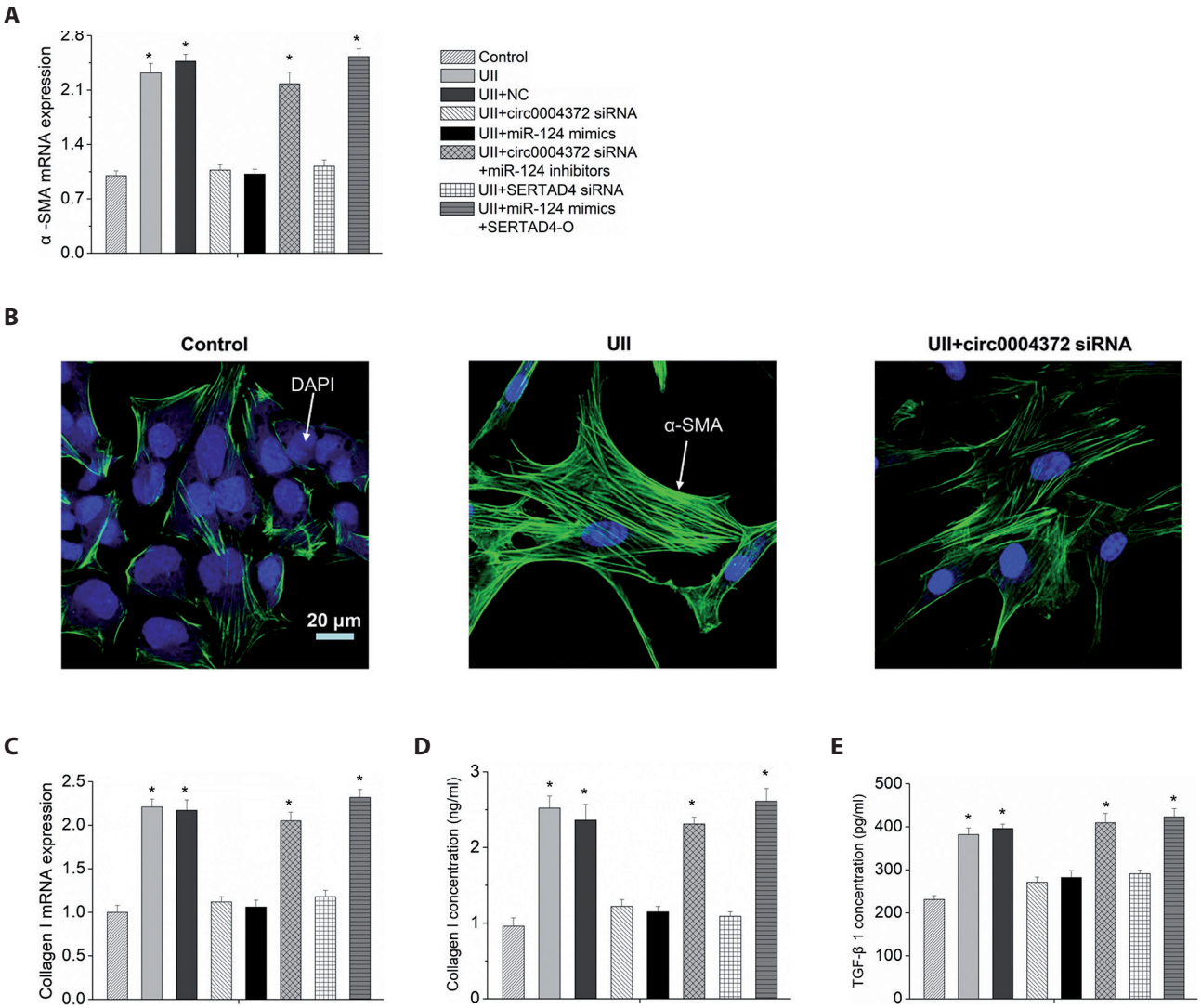

Figure 4. UII promotes VAFs activation through circ0004372/miR-124/SERTAD4 pathway. After transfection and then treatment with UII, the mRNA (**A**) and protein (**B**) expression levels of α-SMA (green color) were detected by qRT-PCR and immunofluorescence staining. The nuclei were stained with DAPI (blue color). The mRNA (**C**) and protein (**D**) expression levels of Collagen I were detected by qRT-PCR and ELISA. The concentration of TGF-β1 (**E**) was detected by ELISA. * $p < 0.05$ *vs.* Control. UII, urotensin II; VAFs, vascular adventitial fibroblasts; NC, negative control. For color figure see online version of the manuscript.

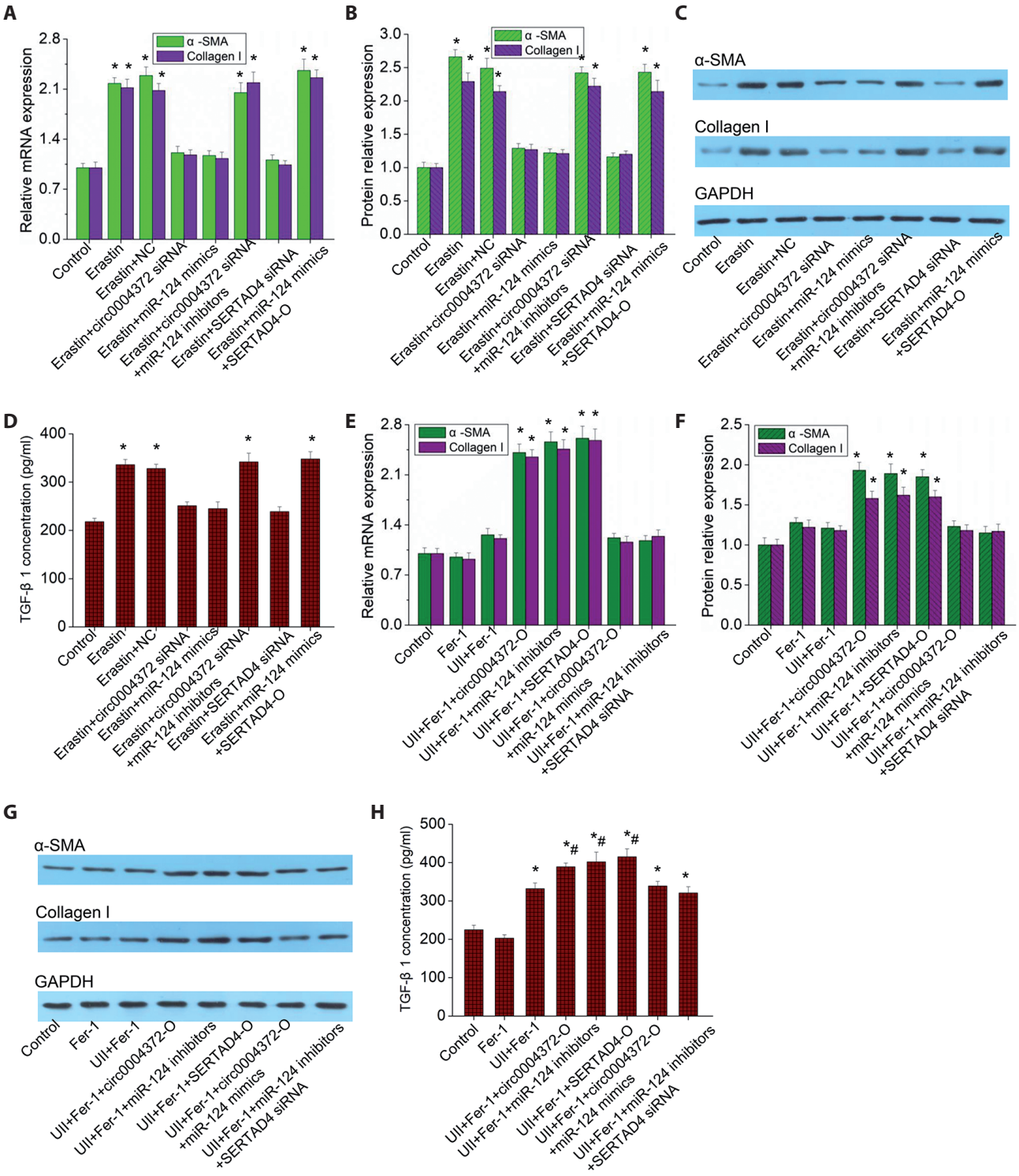

Figure 5. UII promotes VAFs activation by inducing ferroptosis through circ0004372/miR-124/SERTAD4 pathway. After transfection and then treatment with Erastin, the mRNA (**A**) and protein (**B, C**) expression levels of α-SMA and Collagen I were detected by qRT-PCR and Western blot. The concentration of TGF-β1 (**D**) was detected by ELISA. After transfection and then treatment with UII and Ferrostatin-1 (Fer-1), the mRNA (**E**) and protein (**F, G**) expression levels of α-SMA and Collagen I were detected by qRT-PCR and Western blot, and the concentration of TGF-β1 (**H**) was detected by ELISA. * $p < 0.05$ *vs.* Control, # $p < 0.05$ *vs.* UII+Fer-1. For abbreviations, see Figure 1.

activation of VAFs by activating ferroptosis. When UII and Fer-1 were added after transfection with circ0004372 overexpression vector, miR-124 inhibitors or SERTAD4 overexpression vector, the expression of α-SMA, Collagen I and TGF-β1 was still significant; when circ0004372 overexpression vector and miR-124 mimics or miR-124 inhibitors and SERTAD4 siRNA were co-transfected and then UII and Fer-1 were added, the expression of α-SMA, Collagen I and TGF-β1 was not increased significantly (Figure 5E–H). The above results indicate that UII promotes the activation of VAFs through the circ0004372/miR-124/SERTAD4/ferroptosis pathway.

Discussion

VAFs are the main cells of vascular adventitia and play important roles in vascular remodeling. Effectively inhibiting the proliferation, migration and phenotype transformation of VAFs is of great significance for the prevention and treatment of vascular proliferative diseases (An et al. 2015; Tinajero and Gotlieb 2020).

VAFs can be activated into myofibroblasts under the stimulation of various factors, thereby proliferating and migrating to the neointima, secreting extracellular matrix and inflammatory factors, and then participating in the occurrence and development of endothelial hyperplasia and vascular remodeling after vascular injury (An et al. 2015; Tinajero and Gotlieb 2020).

Among various stimulating factors, more and more studies have shown that UII plays an important role in cardiovascular remodeling (Papadopoulos et al. 2008). At the same time, studies have gradually found that UII also plays a role in VAFs (Zhang et al. 2008; Song et al. 2012). For example, Song et al. (2012) found that UII promoted the synthesis of Collagen type I, increased the expression of α-SMA and stimulated the migration of adventitial fibroblasts in a dose-dependent manner. However, there are few studies on the mechanism of UII in VAFs.

It has been found that UII promotes the generation of ROS (Yu et al. 2015), and recent studies have shown that ROS is closely related to ferroptosis, a newly discovered pattern of cell death (Mintz et al. 2020). In this study, UII was used to stimulate VAFs and found that UII activated the ferroptosis pathway, which significantly promoted the production of ROS, MDA and 4-HNE, reduced the activities of SOD, GST and GR, increased the concentration of Fe^{2+}, and inhibited the expression of ferroptosis core regulatory factor GPX4. Ferroptosis is a new way of cell death regulated by various systems *in vivo*. Its occurrence mainly depends on the action of related iron substances *in vivo* and the continuous generation and oxidation of ROS (Mintz et al. 2020). Although UII activated ferroptosis, it promoted AF viability, which may be that UII promotes cell survival by activating other pathways. Zhang et al. (2022) also found that Ang II increased the proliferation and ferroptosis levels of cardiac microvascular endothelial cells at the same time. In addition, UII did not affect AF apoptosis (data not shown), which was consistent with the results of Chen et al. (2014). Chen et al. (2014) showed that UII did not affect the apoptosis of human umbilical vein endothelial cells, but inhibited doxorubicin-induced cell apoptosis.

At present, studies have found that ferroptosis is involved in the progress of various fibrosis and cardiovascular diseases (Gong et al. 2019; Wang et al. 2020). For example, Wang et al. (2019b) found that artemether inhibited the activation of hepatic stellate cells and reduced the formation of fibrotic scars by inducing ferroptosis, thereby significantly reducing liver injury in mouse models of liver fibrosis. In the advanced stage of chronic heart failure, ferroptosis induced by mixed lineage kinase 3 signaling in cardiomyocytes can promote the progression of myocardial fibrosis (Wang et al. 2020). This study found for the first time that UII promoted the activation of VAFs by enhancing ferroptosis, thereby up-regulating the expression of α-SMA and Collagen I. Gong et al. (2019) stimulated HFL1 cells with TGF-β1 and also found that TGF-β1 promoted the expression of α-SMA and Collagen I, increased the levels of ROS and MDA, but inhibited the expression of GPX4, while Erastin further enhanced the above-mentioned effects of TGF-β1, thus it is suggested that ferroptosis plays an important role in the progression of pulmonary fibrosis. Therefore, ferroptosis plays an important role in the activation of a variety of fibroblasts.

Further study on the mechanism of UII showed that UII promoted the expression of circRNA-circ0004372, thereby enhancing ferroptosis and activating VAFs. At present, there have been some research advances on the role of circRNAs in the process of fibrosis and various cardiovascular diseases (Zhu et al. 2021). For example, circHIPK3 expression was significantly up-regulated in hypoxic cardiac fibroblasts, which could act as a sponge of miR-152-3p to promote the expression of TGF-β2, thereby significantly promoting the proliferation, migration and phenotypic transformation of cardiac fibroblasts under hypoxic conditions (Liu et al. 2020). The analysis of circRNA transcriptome in patients with coronary heart disease (CAD) showed that the expression of hsa_circ0001879 and hsa_circ0004104 was significantly up-regulated; their expression levels combined with CAD risk factors could effectively distinguish CAD patients from healthy controls, and overexpression of hsa_circ_0004104 in THP-1-derived macrophages caused dysregulation of atherosclerosis-related genes (Wang et al. 2019a). However, this study is the first to explore the relationship between circRNAs, UII and VAFs. UII enhanced the accumulation of ROS and other factors by promoting the expression of circ0004372, which in turn activated VAFs. Shen et al. (2006) pointed out that Ang II induced VAFs to produce

ROS and then promote the expression of α-SMA, thereby promoting the phenotypic transformation of VAFs to myofibroblasts; reducing the production of ROS inhibited the phenotypic transformation induced by Ang II. Therefore, UII/circ0004372/ROS/ferroptosis pathway may play a key role in the activation of VAFs.

This study further found that UII inhibited the expression of miR-124 through circ0004372, thereby promoting the expression of SERTAD4. The expression of miR-124 in fibroblasts of patients with pulmonary hypertension was significantly reduced, and overexpression of miR-124 in hypertensive fibroblasts significantly reduces the proliferation, migration and the expression of monocyte chemoattractant protein-1 (Wang et al. 2014). Zhang et al. (2017) indicated that up-regulation of miR-124 could inhibit the proliferation of hypertensive pulmonary adventitial fibroblasts, and improve the metabolic function and inflammatory state of cells. This study also had similar findings, indicate that miR-124 plays an inhibitory role in the activation of fibroblasts. Ang II treatment of Human Umbilical Vein Endothelial Cells (HUVECs) led to increased apoptosis, enhanced ROS production and down-regulation of miR-124; up-regulation of miR-124 partially reversed the effect of Ang II on the viability, apoptosis and ROS production of HUVECs by down-regulating the expression of early growth response factor 1 (Lv et al. 2021). ROS is a key factor in triggering ferroptosis, which indicates that miR-124 can affect the process of ferroptosis by regulating oxidative stress. At present, there are few studies on SERTAD4, but Stratton et al. (2019) found that TGF-β induced cardiac fibroblasts to express SERTAD4, which in turn promoted the expression of α-SMA, indicating that SERTAD4 can promote the activation of cardiac fibroblasts. This study also showed that SERTAD4 promoted ferroptosis and then activated VAFs, indicating that SERTAD4 has a key role in the process of fibrosis.

Conclusion

In summary, UII induced circ0004372 expression and inhibited miR-124 expression, thereby promoting SERTAD4 expression in VAFs. Meanwhile, UII significantly increased the accumulation of ROS, MDA and Fe^{2+}, inhibited SOD, GST and GR activities and GPX4 expression, and then promoted the expression of α-SMA, Collagen I and TGF-β1 through circ0004372/miR-124/SERTAD4. Therefore, UII promotes the activation of VAFs through the circ0004372/miR-124/ SERTAD4/ferroptosis pathway. This finding will provide more evidence for the role of VAFs in cardiovascular remodeling and other diseases, thereby providing potential diagnosis and treatment targets.

Funding. This work was supported by the Key R&D Program of Shaanxi Province (No. 2021SF-321).

Conflict of interest. The authors declare that they have no financial conflicts of interest.

References

An SJ, Liu P, Shao TM, Wang ZJ, Lu HG, Jiao Z, Li X, Fu JQ (2015): Characterization and functions of vascular adventitial fibroblast subpopulations. Cell Physiol. Biochem. **35,** 1137-1150 https://doi.org/10.1159/000373939

Chen YL, Tsai YT, Lee CY, Lee CH, Chen CY, Liu CM, Chen JJ, Loh SH, Tsai CS (2014): Urotensin II inhibits doxorubicin-induced human umbilical vein endothelial cell death by modulating ATF expression and via the ERK and Akt pathway. PLoS One **9,** e106812 https://doi.org/10.1371/journal.pone.0106812

Ding S, Zhu Y, Liang Y, Huang H, Xu Y, Zhong C (2018): Circular RNAs in vascular functions and diseases. Adv. Exp. Med. Biol. **1087,** 287-297 https://doi.org/10.1007/978-981-13-1426-1_23

Gong Y, Wang N, Liu N, Dong H (2019): Lipid peroxidation and GPX4 inhibition are common causes for myofibroblast differentiation and ferroptosis. DNA Cell Biol. **38,** 725-733 https://doi.org/10.1089/dna.2018.4541

Kristensen LS, Andersen MS, Stagsted LVW, Ebbesen KK, Hansen TB, Kjems J (2019): The biogenesis, biology and characterization of circular RNAs. Nat. Rev. Genet. **20,** 675-691 https://doi.org/10.1038/s41576-019-0158-7

Liu W, Wang Y, Qiu Z, Zhao R, Liu Z, Chen W, Ge J, Shi B (2020): CircHIPK3 regulates cardiac fibroblast proliferation, migration and phenotypic switching through the miR-152-3p/TGF-β2 axis under hypoxia. PeerJ **8,** e9796 https://doi.org/10.7717/peerj.9796

Lu QB, Wang HP, Tang ZH, Cheng H, Du Q, Wang YB, Feng WB, Li KX, Cai WW, Qiu LY, et al. (2018): Nesfatin-1 functions as a switch for phenotype transformation and proliferation of VSMCs in hypertensive vascular remodeling. Biochim. Biophys. Acta Mol. Basis Dis. **1864,** 2154-2168 https://doi.org/10.1016/j.bbadis.2018.04.002

Lv L, Shen J, Xu J, Wu X, Zeng C, Lin L, Mao W, Wei T (2021): MiR-124-3p reduces angiotensin ii-dependent hypertension by down-regulating EGR1. J. Hum. Hypertens. **35,** 696-708 https://doi.org/10.1038/s41371-020-0381-x

Mintz J, Mirza J, Young E, Bauckman K (2020): Iron therapeutics in women's health: Past, present, and future. Pharmaceuticals (Basel) **13,** 449 https://doi.org/10.3390/ph13120449

Papadopoulos P, Bousette N, Giaid A (2008): Urotensin-II and cardiovascular remodeling. Peptides **29,** 764-769 https://doi.org/10.1016/j.peptides.2007.09.012

Pasterkamp G, de Kleijn DP, Borst C (2000): Arterial remodeling in atherosclerosis, restenosis and after alteration of blood flow: Potential mechanisms and clinical implications. Cardiovasc. Res. **45,** 843-852 https://doi.org/10.1016/S0008-6363(99)00377-6

Sekaran NK, Crowley AL, de Souza FR, Resende ES, Rao SV (2017): The role for cardiovascular remodeling in cardiovascular outcomes. Curr. Atheroscler. Rep. **19,** 23

https://doi.org/10.1007/s11883-017-0656-z
Shen WL, Gao PJ, Che ZQ, Ji KD, Yin M, Yan C, Berk BC, Zhu DL (2006): NAD(P)H oxidase-derived reactive oxygen species regulate angiotensin-ii induced adventitial fibroblast phenotypic differentiation. Biochem. Biophys. Res. Commun. **339,** 337-343
https://doi.org/10.1016/j.bbrc.2005.10.207
Song N, Ding W, Chu S, Zhao J, Dong X, Di B, Tang C (2012): Urotensin II stimulates vascular endothelial growth factor secretion from adventitial fibroblasts in synergy with angiotensin II. Circ. J. **76,** 1267-1273
https://doi.org/10.1253/circj.CJ-11-0870
Stratton MS, Bagchi RA, Felisbino MB, Hirsch RA, Smith HE, Riching AS, Enyart BY, Koch KA, Cavasin MA, Alexanian M, et al. (2019): Dynamic chromatin targeting of BRD4 stimulates cardiac fibroblast activation. Circ. Res. **125,** 662-677
https://doi.org/10.1161/CIRCRESAHA.119.315125
Tinajero MG, Gotlieb AI (2020): Recent developments in vascular adventitial pathobiology: The dynamic adventitia as a complex regulator of vascular disease. Am. J. Pathol. **190,** 520-534
https://doi.org/10.1016/j.ajpath.2019.10.021
Wang D, Zhang H, Li M, Frid MG, Flockton AR, McKeon BA, Yeager ME, Fini MA, Morrell NW, Pullamsetti SS, et al. (2014): Microrna-124 controls the proliferative, migratory, and inflammatory phenotype of pulmonary vascular fibroblasts. Circ. Res. **114,** 67-78
https://doi.org/10.1161/CIRCRESAHA.114.301633
Wang J, Deng B, Liu Q, Huang Y, Chen W, Li J, Zhou Z, Zhang L, Liang B, He J, et al. (2020): Pyroptosis and ferroptosis induced by mixed lineage kinase 3 (MLK3) signaling in cardiomyocytes are essential for myocardial fibrosis in response to pressure overload. Cell Death Dis. **11,** 574
https://doi.org/10.1038/s41419-020-02777-3
Wang L, Shen C, Wang Y, Zou T, Zhu H, Lu X, Li L, Yang B, Chen J, Chen S, et al. (2019a): Identification of circular RNA Hsa_circ_0001879 and Hsa_circ_0004104 as novel biomarkers for coronary artery disease. Atherosclerosis **286,** 88-96
https://doi.org/10.1016/j.atherosclerosis.2019.05.006
Wang L, Zhang Z, Li M, Wang F, Jia Y, Zhang F, Shao J, Chen A, Zheng S (2019b): P53-dependent induction of ferroptosis is required for artemether to alleviate carbon tetrachloride-induced liver fibrosis and hepatic stellate cell activation. IUBMB Life **71,** 45-56
https://doi.org/10.1002/iub.1895
Yu X, Wang P, Shi Z, Dong K, Feng P, Wang H, Wang X (2015): Urotensin-II-mediated reactive oxygen species generation via NADPH oxidase pathway contributes to hepatic oval cell proliferation. PLoS One **10,** e0144433
https://doi.org/10.1371/journal.pone.0144433
Zhang H, Wang D, Li M, Plecitá-Hlavatá L, D'Alessandro A, Tauber J, Riddle S, Kumar S, Flockton A, McKeon BA, et al. (2017): Metabolic and proliferative state of vascular adventitial fibroblasts in pulmonary hypertension is regulated through a microrna-124/PTBP1 (polypyrimidine tract binding protein 1)/pyruvate kinase muscle axis. Circulation **136,** 2468-2485
https://doi.org/10.1161/CIRCULATIONAHA.117.028069
Zhang YG, Li J, Li YG, Wei RH (2008): Urotensin II induces phenotypic differentiation, migration, and collagen synthesis of adventitial fibroblasts from rat aorta. J. Hypertens. **26,** 1119-1126
https://doi.org/10.1097/HJH.0b013e3282fa1412
Zhang YG, Hu YC, Mao YY, Wei RH, Bao SL, Wu LB, Kuang ZJ (2010): Transforming growth factor-β1 involved in urotensin II-induced phenotypic differentiation of adventitial fibroblasts from rat aorta. Chin. Med. J. (Engl) **123,** 3634-3639
Zhang Z, Tang J, Song J, Xie M, Liu Y, Dong Z, Liu X, Li X, Zhang M, Chen Y, Shi H, Zhong J (2022): Elabela alleviates ferroptosis, myocardial remodeling, fibrosis and heart dysfunction in hypertensive mice by modulating the IL-6/STAT3/GPX4 signaling. Free Radic. Biol. Med. **181,** 130-142
https://doi.org/10.1016/j.freeradbiomed.2022.01.020
Zhu L, Li N, Sun L, Zheng D, Shao G (2021): Non-coding RNAs: The key detectors and regulators in cardiovascular disease. Genomics **113,** 1233-1246
https://doi.org/10.1016/j.ygeno.2020.10.024
Zou M, Huang C, Li X, He X, Chen Y, Liao W, Liao Y, Sun J, Liu Z, Zhong L, et al. (2017): Circular RNA expression profile and potential function of hsa_circRNA_101238 in human thoracic aortic dissection. Oncotarget **8,** 81825-81837
https://doi.org/10.18632/oncotarget.18998

Received: September 15, 2021
Final version accepted: May 27, 2022